

Explainable Artificial Intelligence in Process Mining: Assessing the Explainability-Performance Trade-Off in Outcome-Oriented Predictive Process Monitoring

Alexander Stevens^{a,*}, Johannes De Smedt^a

^a*KU Leuven Research Centre for Information Systems Engineering (LIRIS), Naamsestraat 69, 3000 Leuven, Belgium*

Abstract

Recently, a shift has been made in the field of Outcome-Oriented Predictive Process Monitoring (OOPPM) to use models from the eXplainable Artificial Intelligence paradigm, however the evaluation still occurs mainly through performance-based metrics not accounting for the implications and lack of actionability of the explanations. In this paper, we define explainability by the interpretability of the explanations (through the widely-used XAI properties parsimony and functional complexity) and the faithfulness of the explainability model (through monotonicity and level of disagreement). The introduced properties are analysed along the event, case, and control flow perspective that are typical of a process-based analysis. This allows to quantitatively compare, *inter alia*, inherently created explanations (e.g., logistic regression coefficients) with post-hoc explanations (e.g., Shapley values). Moreover, this paper contributes a guideline named X-MOP to practitioners to select the appropriate model based on the event log specifications and the task at hand, by providing insight into how the varying preprocessing, model complexity and post-hoc explainability techniques typical in OOPPM influence the explainability of the model. To this end, we benchmark seven classifiers on thirteen real-life events logs.

Keywords: Explainable AI (XAI), Predictive Process Monitoring, Interpretability, Faithfulness, Deep Learning, Machine Learning

*Corresponding author: alexander.stevens@kuleuven.be

1. Introduction

Business processes are the arterial systems that define modern organizations and their information systems [1]. The analysis of processes through data-driven approaches is labelled as process mining [2] and has seen a strong uptake. Among the wide range of techniques available, the focus of this study lies with predictive process monitoring [3], the umbrella term primarily geared towards predictive activities. It allows identifying process-related trends regarding particular goals (e.g., will customers be awarded credit?), impeding bottlenecks and whether particular activities will occur in the future. In the case of Outcome-Oriented Predictive Process Monitoring (OOPPM), the concrete objective is to predict the future state of an incoming, incomplete case. Hence, it is important that this is done as accurately as possible. An often anticipated trend is to increase the predictive performance by focusing on representation learning [4, 5, 6, 7], or on the introduction of computationally complex models such as ensemble models [4, 3], deep neural networks [8, 9, 10], and many more [11]. However, the increased accuracy and flexibility of these black boxes induces the inability to link the output back to the original inputs and therefore consequently inhibits to understand the model behaviour.

In response to this, the field of Explainable AI focuses on gaining insights into ‘how’ and ‘why’ certain predictions in complex structures were made, while trying to maintain the predictive performance of these highly performant models [12]. Nonetheless, many XAI proponents such as Rudin [13] state that trying to explain these complex models comes with a loss of faithfulness, due to the fact that the relationship between input and output can only be approximated [13, 14, 15]. Nonetheless, the use of increasingly complex models has been widely adopted in high stake decision-making processes throughout society. [16, 17].

This paper identifies three main issues that arise in the intersection of OOPPM

and XAI. First, the existing research is constrained to the computational aspects while neglecting the interpretation, actionability, and implications of the results. Second, it is crucial that the explanations in the context of business process monitoring are made in a faithful and interpretable way, as the main focus of this field is to verify its conformance with respect to the business requirements and goals [18, 19, 2]. In [20], they state that domain-specific metrics guide the practitioners to select the best model for the task at hand. Third, a more comprehensive study about the faithfulness and interpretability of XAI techniques in OOPPM is hence missing.

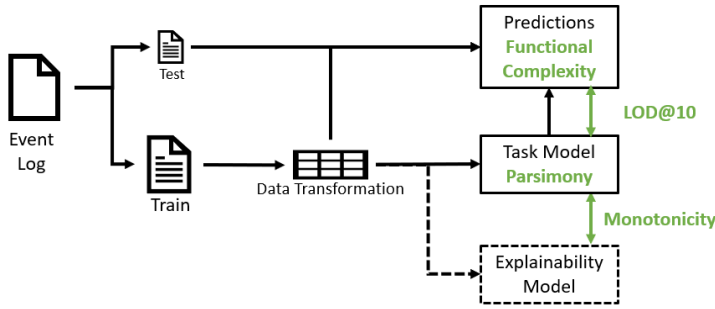


Figure 1: The proposed framework to calculate explainability metrics for explainable AI purposes in OOPPM

This paper tackles these issues through three contributions. First, this paper introduces a comprehensive basis for Explainable AI in OOPPM by formulating a framework of metrics as shown in Fig. 1. Second, a benchmarking study is performed with five machine learning and two deep learning algorithms, with the former models preprocessed in two different ways. In this sense, this paper is complementary with the study of Teinemaa [3] and Kratsch [8] by comparing the experimental set-up with both deep learning and newly-introduced interpretable models. Third, we provide a framework based on an extensive set of guidelines to obtain accurate and explainable OOPPM solutions based on a wide benchmark of traditional machine learning, deep learning, preprocessing and explainability approaches for OOPPM. In a nutshell, we show that each

model has its advantages and disadvantages, and that the requirements imposed by the stakeholders are important in order to arrive at the ideal model for the task at hand, as naively opting for the model with the highest predictive performance can have a strong detrimental effect on both the interpretability of explanations and the faithfulness of an explainability models. Next, the revisited explainability-predictive accuracy trade-off demonstrates that the faithful Generalized Logistic Rule Model (GLRM) model exhibits high interpretability, for only a small loss of performance. The results are evaluated on 13 event logs. This work extends the initial work of [paper removed to ensure anonymization], on metrics which allow comparing inherently created explanations with post-hoc explanations in the context of OOPPM. The rest of the paper is organized as follows: First, a review of the literature regarding explainability in predictive process monitoring is given in Section 2, together with the motivation for this line of research. This is followed by preliminaries defined in Section 3. Next, a definition for explainability is given, together with the introduced metrics in Section 4. The benchmark study and implementation details can be found in Section 5, after we clarify the research questions in Subsection 5.1. In Section 6, the insights obtained from the research questions are incorporated into a framework of guidelines that allow to obtain eXplainable models and Metrics in Outcome-oriented predictice Process Monitoring (X-MOP). Finally, the results and obtained insights are concluded in Section 7.

2. Related Work and Motivation

Predictive process monitoring is concerned with the early prediction of the future state of an ongoing case. Predictive efforts are primarily driven by using machine learning models such as XGBoost [3, 21, 22], random forest [8, 23, 3], support vector machines [8, 3] or logistic regression (LR) [3], with recent works showing interest in applying deep learning models [24, 25]. A wide range of works have already evaluated these different models with performance-based metrics [3, 8, 26]. Over the last two years, there has also been a lot of movement

around explainability in predictive process monitoring [23, 27, 22, 28, 29, 30, 11, 19]. Related to the XAI literature [13], these different works can be divided into two different trends based on how they deal with the explainability-accuracy trade-off.

The first trend presumes the complex model as the *task model* [14] and looks for explanations using post-hoc techniques. In predictive process monitoring, several papers have already suggested model-agnostic explainability techniques on top of machine learning models [23, 22] such as SHapley Additive exPlanations (SHAP) [31] or Local Interpretable Model-Agnostic Explanations (LIME) [32], with similar developments in a deep learning context [27, 30, 33, 28, 29]. In [27], an LSTM model in combination with SHAP values allow the user to identify the influence of certain attributes in the different steps of the process, while Mehdiyev focuses on creating local post-hoc explanations with the use of a surrogate decision tree [30]. In [33] and [28], they use a Bidirectional LSTM (one forward RNN and one backward RNN), where after the hidden states of the time steps of both RNNs are concatenated. Moreover, a context vector is learnt that takes the different time steps into account. In addition, [29] visualizes the impact of the activities on the predictions with the use of gated graph neural networks.

The second trend introduces interpretable models instead of trying to break open these black box models. Furthermore, they state that there are alternative models available, often through performance-maximization, that yield better explainability-performance trade-offs. In [34], a set of fuzzy rules are learnt from neural networks. Moreover, the relationship between inputs and output is explained by a set of IF-THEN rules. the use of domain knowledge is needed for binning the attributes into different 'interpretable' terms. Next, a Bayesian network is used in [11] for next event and suffix prediction. Even though the causal relationships are inferred from historical data, it relies on assumptions of domain knowledge [12]. Finally, [35] introduces two models to OOPPM, i.e., Logit Leaf Model (LLM) and Generalized Logistic Rule Model (GLRM), both drawn from XAI literature and adapted to the OOPPM case.

It has already been pointed out that the post-hoc explainability techniques should uncover, apart from an interpretable explanation, the *true reasons* for model predictions [14, 15, 36]. Many papers have already investigated the unfaithfulness of post-hoc explainability models [37, 21, 38, 36]. A recent study by Ma [37] has suggested that there was a non-monotonic relationship between the SHAP values and the predictive performance. Similarly, Velmurugan [21] investigated the faithfulness of SHAP versus LIME based on perturbations, reporting low-to-moderate faithfulness scores. The use of an attention mechanism to interpret the importance of attributes has also been questioned [36, 38]. In [36] the findings show that, generally speaking, the highest attention weights mostly do have a higher attribute importance compared to an attribute with a low attention score, the ranking of the attention importance scores is not faithful to the model decisions. Similarly, the work of Jain and Wallace [38] states that the learned attention weights are mostly uncorrelated with the gradient-based attribute importance, even though they mimic the predictions rather accurately. Although these studies are already shedding some light in the dark (read: an attempt to quantify how ‘unfaithful’ the current post-hoc explainability techniques are), other papers introduced quantitative metrics to assess the quality of explanation methods [39, 15, 40]. Islam [40] created a metric for explainability based on different specified properties, while [39] introduces a metric based on three different properties that define the model complexity. However, these metrics do not take the faithfulness of the explainability model into account, Nguyen [41] advises to use mutual information to describe the faithfulness of the explanation, but this metric can not be calculated for all explainability models (i.e. are not model agnostic). Likewise, [15] introduced many (mostly model-agnostic) quantitative metrics based on the identified properties for explainability.

A comprehensive study about the unfaithfulness is missing due to a number of reasons. First, the accuracy by which these post-hoc explanations reflect the effective model behaviour of the predictive model is often inadequate in terms of attribute space [13, 35]. Second, [17] states that correlated attributes

within a dataset can lead to unfaithful explanations if there are many correlated attributes in the dataset. Third, other work demonstrates that there is a non-monotonic relationship between the SHAP values and the predictive performance [37].

These works illustrate that there is a growing need for consistent evaluation based on non-performance metrics such as explainability, which includes both the *faithfulness of the explainability technique* and *interpretability of the explanations*. Both are important prerequisites to ensure that implications made of the results are correct and actionable. This means that, even if the faithfulness of the explainability technique is uncompromised, the interpretability of the explanation is questioned when it is based on e.g. 500 attributes [42]. In addition, these metrics would reduce the scope of research for human-based studies by reducing the financial and time costs of such experiments. There is a notable void in the OOPPM literature in this respect, which this paper will address through both introducing the notions of interpretability, faithfulness, as well as a OOPPM-specific set of guidelines.

3. Preliminaries

This section first describes the different terminology inherited from the XAI field, followed by the preliminary steps needed for predictive process monitoring purposes.

3.1. The different XAI nomenclatures

Task model As already mentioned in Section 1, several studies have defined the (complex) model that generates the predictions as the *task model* [14, 13].

Transparency. In the literature, *transparency* is often described as the opposite of *blackbox-ness* [12]. Furthermore, a transparent model (also named interpretable model) is a task model that is able to generate its own explanations, where the black box model requires the need of an additional explainability model.

Interpretability. Originally described as *comprehensibility* in [12], is the ability to provide an explanation that consists out of single chunks of information, in a human understandable fashion. Furthermore, it is often quantified by the related concept of model complexity [12, 39].

Explainability model. An explainability model is the umbrella term for the post-hoc explainability techniques that exist to generate explanations for a black box model such as surrogate models [30], attention layers [28] and SHAP values [43]. Previous research has mostly referred to this as *post-hoc explanations* [14, 12], or *post-hoc interpretations* [39]. Here, the term *explainability model* is used to indicate that the post-hoc explainability techniques should be both interpretable and *faithful* (see *infra*).

Faithfulness. The faithfulness of an explainability model can be considered as the accuracy by which the explainability model accurately mimics the behaviour of the task model (and **not** the predictions of the task model), as similar predictions do not ensure that it correctly mimicked the behaviour of the task model [13]. Note that the explainability model of an interpretable model is the task model itself.

Explainability. Even though often used interchangeably [12], interpretability and explainability differ significantly due to the fact that understanding the explanations of the task model is different from the ability to link the inputs with its predicted output in a faithful way. Moreover, an explanation should be both interpretable and faithful, where the latter is compromised if the effective behaviour of the model is accurately represented. To emphasize, a simple explanation generated for a rain forecast prediction could be: ‘*if the grass is green, it will rain*’, which is easy to interpret, but unfaithful. The necessity to distinguish between faithfulness and interpretability has already been pointed out by prior research [14, 15].

3.2. OOPPM setup

OOPPM relies on the use of historic process data recorded in an event log, which is a list of traces that represents the enactment of a process for a partic-

ular case within an information system [44]. Moreover, a trace is considered a sequence of timestamped events generated by executing a particular activity in the process. An event is a tuple of d attributes $x'_{j,j \in \{1, \dots, d\}}$ such as an activity name, Case ID, timestamp, and so on. Thus, each event has a corresponding activity label, as well as other event-related attributes which change during the course of the case (dynamic attributes, sometimes also referred to as *payload attributes*). Some attributes do not evolve during the execution of a single case and are called case attributes (or static attributes).

The first transformation step extracts (trace) prefixes from the completed cases to be able to learn, preferably incrementally, from the development of the traces. To this end, a prefix log is typically derived, which is the extracted event log that contains all the prefixes of each case in the original event log. Next, trace cutting is often done when the distribution of the output label is disproportionately distributed over longer prefixes, or for computational reasons [45].

The second data transformation step describes the encoding mechanism that enables the user to work with a varying amount of attributes, since each trace can have a different length. In the work of van Dongen [46], the focus is on the order and execution of the activity in the trace (i.e. control flow encoding), with further research in predictive monitoring [5, 47, 3] advising to expand the attribute space with other event and case attributes (i.e. data payload encoding).

An often used encoding mechanism is the aggregation encoding technique [6].

First, the categorical static attributes are one-hot encoded, which means that each categorical static attribute x'_j results in a number of transformed attributes based on the unique attribute values $\theta(x'_j)$, with $\theta(x'_j) = \{x'_{i,j}\}_{i \in \{1, \dots, n\}}$. The numeric static attributes remain unchanged. Second, the dynamic numeric attributes are replaced by their summary statistics *min*, *max*, *mean*, *sum* and *std*. The last transformation step relates to the dynamic categorical attributes, where the frequency of occurrence of an attribute value in a prefix is the value for the new attribute.

To overcome the obvious drawbacks of the aggregation encoding, the idea of

index encoding [5, 3] is to use all possible information in the trace, including the order of the trace. First, a categorical event attribute generates a number of attributes with a factor similar to the number of attribute values multiplied with the prefix length. Note that only for the activity values that actually happened (i.e. visible in the event log), a new index is created. Second, the amount of case attributes remain unchanged compared to the aggregation encoding due to their static nature. This way, a lossless encoding of the trace is achieved, which means that it is possible to completely recover the original trace based on its attribute vector.

By contrast, the use of the above encoding mechanism in step-based models such as recurrent neural networks becomes superfluous given their sequential setup. To exploit this efficiently, a low-dimensional representation of discrete attributes in the form of embeddings is an often performed encoding technique [10]. This mapping transforms the categorical attribute to a vector of continuous numbers, similarly to how one-hot encoding works. Nonetheless, the latter ignores the similarity between the obtained vectors.

In the next part of this paper, the attributes $x_{j,j \in \{1, \dots, p\}}$ are the resulting attributes after the data transformation steps, performed on the train event log. Consequently, the value for prefix $i, i \in \{1, \dots, n\}$ on attribute $x_{j,j \in \{1, \dots, p\}}$ is denoted by $x_{i,j}$.

Trace bucketing is a commonly used technique to support the discovery of heterogeneous segments in the data. First, techniques such as K-Nearest Neighbours [47] or K-Means clustering measure the (dis)similarity between traces depending on the parameter K. Second, prefix bucketing [5] creates different buckets (and consequently different models) for the prefixes of different lengths. Third, the state-based bucketing technique [48] creates a different model for each different decision point within the process model. However, while bucketing can effectively diminish the runtime performance [3], the clustering does not necessarily result in an intuitive or interpretable outcome. E.g., clustering techniques can base their grouping on a high number of dimensions that are not interpretable. Furthermore, there is no guarantee that the use of a bucketing

technique will effectively improve performance. These insights were obtained and tested in [6].

After the data transformation steps, the transformed event log is used to create a *classifier* to predict the dependent variable based on independent attributes. Moreover, the prediction for prefix trace i is denoted as $\hat{y}_i = F(x_{i,1}, \dots, x_{i,p})$. The final step is to interpret the predictions made. In the one hand, in a transparent model, the inherently estimated coefficients $w_{a,1}, \dots, w_{a,p}$ of a transparent model indicate the importances of the different attributes on the dependent variable. Fig. 1 therefore only needs to be taken into account when the predictive model is a black box model that requires the need of an additional explainability technique. In the other hand, the use of a (post-hoc) explainability model is often considered to approximate the attribute weights of the black box model (i.e. task model) with the attribute weights $w_{e,1}, \dots, w_{e,p}$ of the explainability model.

4. Explainability in OOPPM

The necessity to distinguish between faithfulness and interpretability was already stated in [14, 15]. and is adapted in this paper for OOPPM purposes. As a result, 2 shows that the combination of *interpretability of explanations* and *faithfulness of explainability model* allows quantifying and thus evaluating explainability. To calculate the interpretability of an explanation in the OOPPM context, it is necessary to divide the attributes into their different types: case, event and control flow attributes.

An *interpretable model* is different from the *interpretability of the explanation*. Moreover, an interpretable model (e.g. logistic model) that creates its own explanations based on more than 500 attributes [42], has a low value for interpretability of explanation. In this sense, a deep neural network (i.e. a non-interpretable model) can have higher interpretability of explanations compared to a logistic regression model. The XAI explainability-accuracy trade-off compares the model interpretability (and not *interpretability of explanation*) with the model

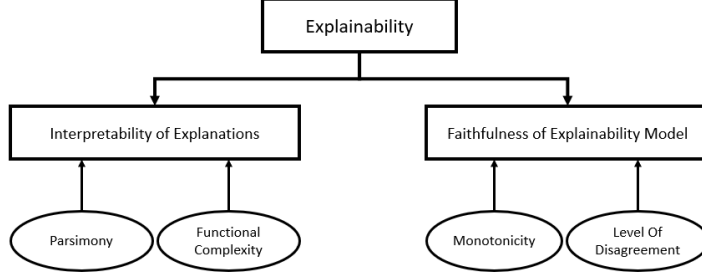


Figure 2: Explainability definition

accuracy, assuming that it is required to strike a balance between either simple models (e.g. linear regression) or models using complex inference structures (e.g. neural networks). This paper investigates whether the *interpretability of an explanation* is also in trade-off with the *accuracy*.

Note that, in the case of an interpretable model, the interpretable model generates its own explanations. Therefore, the faithfulness of the *explainability mode* is 1 by definition.

4.1. Quantitative Metrics

Parsimony is a property of interpretability [42] that represents the complexity of a model [14], an often used metric for linear models. Moreover, the parsimony C of a model F , C_F , is quantified by the number of attributes in the resulting model. This can be seen as the number of attributes with non-zero weights e.g., linear regression coefficients with a corresponding weight different from 0, in other cases the non-zero weights provided by the post-hoc attribute importance. Since the focus is on the interpretability of the explanation, we define the parsimony of the model as a property for the *interpretability of an explanation* rather than a property for *model interpretability*. The parsimony of the total model maximally equal to the sum of the amount of attributes of each type t . Moreover, a parsimonious (i.e. simple) model corresponds to a low value for $C_F = C_{event} + C_{case} + C_{control}$.

Assume attribute $x_{j,k}$ with $w_{j,k}$ the weight of an attribute $x_j, j \in \{1 \dots p\}$

in the model F , with attribute type $t \in \{1 \dots k\}$. Then, the total parsimony C_F is calculated as follows:

$$C_F = \sum_{k=1}^t \sum_{j_k=1}^{p_k} C(x_{j,k}) \quad (1)$$

with

$$C(x_{j,k}) = \begin{cases} 1, & \text{if } w_{j,k} > 0, \\ 0, & \text{otherwise.} \end{cases} \quad (2)$$

Functional Complexity is, alongside parsimony, a metric of model complexity. This permutation-based metric (originally named *number of features used* in [39]) initially determined *if any* of the predictions change when the values $x_{i,j, i \in \{1, \dots, m\}}$ for the attribute x_j are permuted. Additionally, [49] states that small random perturbations to the test images can drastically change the (attention-based) explanations, without the predicted label being flipped. Therefore, we adapt this metric to retrieve the dependency of the attribute types (i.e., event/case/control flow) on the explanations by investigating how much percent of the predictions are flipped. The Functional Complexity (FC) is calculated on the test data, and is therefore useful to verify *how many* different predictions there would be when permuting the attribute values of an attribute type, and consequently measures how strongly the explanations depend on that attribute type.

Assume $\hat{y}^* = F(x_{1,1}, \dots, x_{i,j}^*, \dots, x_{i,j+k}^*, \dots, x_{m,p})$ as the prediction after permutation for attribute type t , where $x_{i,j}^*, \dots, x_{i,j+k}^*$ are the permuted attribute values of the attribute x_j, \dots, x_{j+k} of the test instance i . In Algorithm 1, the pseudocode of how the permutations are made in order to obtain the FC values for the different attribute types, is given. The algorithm starts by selecting the attributes of a certain attribute type (*lines 3-5*), with the attribute value of instance i for attribute x_j removed from the set of permuted values in *line 10*. The functional complexity of an attribute type is calculated as the amount of prediction changes before (*line 16*) and after (*line 17*) permuting all the at-

tributes of an attribute type t , divided by the number of instances. Finally, the Hamming Distance (*line 18*) is used as the distance measure, where a low value for FC_t means that the predictions are created seemingly independently of this attribute type and should therefore not be regarded as an important attribute type when interpreting the explanations.

Algorithm 1 Functional Complexity

Require: $x_{1,1}, \dots, x_{1,p}, \dots, x_{m,1}, \dots, x_{m,p}$

Ensure: $FC_{event}, FC_{case}, FC_{control}$

```

Attributetypes  $\leftarrow [event, case, control]$ ,  $FC_{event} \leftarrow 0, FC_{case} \leftarrow 0, FC_{control} \leftarrow 0, z \leftarrow ()$ 
Test  $\leftarrow [x_{1,1}, \dots, x_{1,p}, \dots, x_{m,1}, \dots, x_{m,p}]$   $\triangleright$  To make the pseudocode simpler
3: for  $t \in \text{Attributetypes}$  do
     $Test_{copy} \leftarrow \text{Copy}(Test)$   $\triangleright$  copies the test data for each attribute type  $t$ 
    for  $j \in \text{Attributes}$  do  $\triangleright$  take only the attributes of type  $t$ 
        6:  $NewValues \leftarrow ()$ 
         $z \leftarrow \theta(Test[j])$   $\triangleright$  all the unique attribute values of that attribute
        for  $i \in \text{Instances}$  do
            9:  $Value = Test[i, j]$   $\triangleright$  the current attribute value of instance  $i$ 
             $z^* \leftarrow \{x \in z : x \notin Value\}$   $\triangleright$  remove the current value
            if  $\text{length}(z^*) \leq 1$  then
                12:  $NewValues[i, j] \leftarrow Value$   $\triangleright$  for static attributes
            else
                 $NewValues[i, j] \leftarrow \text{Random}(z^*)$   $\triangleright$  take a random value
            15:  $Test_{copy}[i, j] \leftarrow NewValues$   $\triangleright$  replace with the permuted attribute values
             $\hat{y}_i = F(Test)$ 
             $\hat{y}^* = F(Test_{copy})$   $\triangleright$  predictions after permuting attributes of type  $t$ 
            18:  $FC_t \leftarrow \frac{\text{distance}(\hat{y}, \hat{y}^*)}{n}$   $\triangleright$  a different FC for each attribute type  $t$ 

```

Monotonicity (M) is the notion that describes how faithful the attribute importance ranking of the explainability model is to the ranking made by the task model. By definition, monotonicity is ensured (i.e. $M = 1$) if the model inherently generates its own explanations [13]. We quantify the monotonicity of a post-hoc explainability model by the non-parametric Spearman's correlation coefficient, similarly to [41, 49].

$$M = \rho(w_a, w_e)$$

with $w_a = w_{a,1}, \dots, w_{a,p}$ the attribute weights of the task model and $w_e = w_{e,1}, \dots, w_{e,p}$ the weights of the explainability model. This correlation coefficient is a non-parametric measure that takes a value between [-1,1] and describes the association of rank. A perfectly faithful model has a correlation coefficient of +1, where a loss in faithfulness corresponds with a value closer to 0. Consequently, a negative value corresponds to a negative rank association between the two attribute importance weights.

Level Of Disagreement (LOD@10) [50] originally computes the percentage of similar predictions between the task model and post-hoc explanations. In this paper, the LOD@10 compares the top ten importance of the attribute types of the task model with the attributes of the explainability model. The LOD@10, different from monotonicity, neglects the ranking of the attributes but looks at the relative frequency of the attribute types. Moreover, the metric is quantified with the Euclidean Distance between the relative frequency of top ten attributes of the task model $\#_{a,k}$ and the explainability model $\#_e$,

$$LOD@10 = d(\#_a, \#_k) = \sqrt{\sum_{k=1}^t (\#_{a,k} - \#_{e,k})^2} \quad (3)$$

and

$$\begin{cases} \# \sum_{k=1}^t \#_{a,k} = 10, \\ \# \sum_{k=1}^t \#_{e,k} = 10. \end{cases} \quad (4)$$

which indicates if the explainability model has focused on similar attribute types compared to the task model. This metric is introduced to take into account that the number of attributes used in the task model has a negative influence on the monotonicity value. Furthermore, a high value for this LOD@10 metric indicates that the explainability model focused on rather different attribute types, which impairs the faithfulness of the explainability model.

5. Benchmark study

In this section, a detailed build-up to the research questions is provided to demonstrate how the introduced metrics can guide the stakeholders into obtaining interpretable and faithful OOPPM models. Next, the event logs and their specifications are described, followed by the benchmark. Finally, the hyper optimization settings and implementation details of the different models are given.

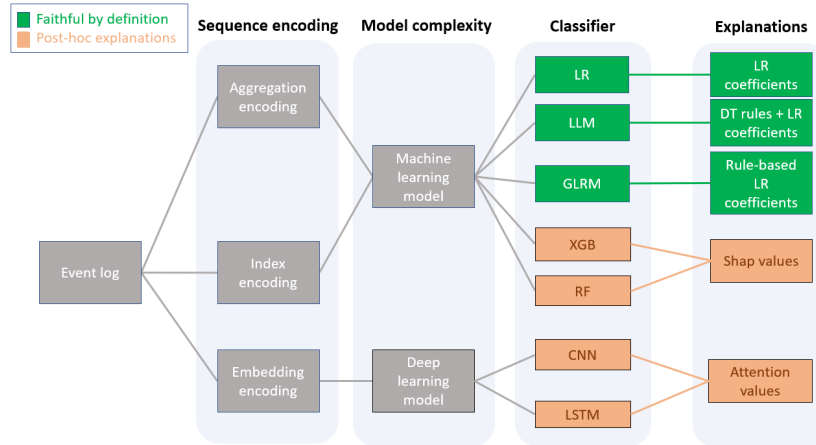


Figure 3: Overview of experimental pipeline. The interpretable models (and generated explanation methods) are indicated in green. The black box models, that require post-hoc explanations, are coloured in orange.

5.1. Research Questions

As mentioned before, the goal is to uncover a set of guidelines to obtain accurate and explainable OOPPM solutions. Therefore, this benchmarking study investigates the influence of the most important steps in an OOPPM context, on the *explainability of the explanations* and the *faithfulness of the explainability model*. The experimental pipeline is similar to the benchmark studies of [3] and [8] and extended with an XAI dimension (see Fig. 3). The evaluation is performed with the explainability metrics of Section 4.1.

First, this study aims to uncover the influence that sequence encoding techniques

(see Fig. 3) have on both the interpretability and faithfulness of OOPPM models, as this encoding is an integral part of transforming process data. This leads to the first research question, *RQ1*.

Second, recurrent neural networks, due to their inherent sequential architecture, are able to model time-dependent and sequential data tasks without such aggregation. On the other hand, it has also been shown that CNNs outperform LSTM for sequential data predictions [34, 51]. The next two research questions *RQ2* and *RQ3* discuss the model complexity and aim to assess whether the deep learning model focus more on the control flow perspective, and whether the previously established outperformance of the deep learning models [8] comes at the cost of interpretability and/or faithfulness.

Next, this study compares the LLM model, introduced in [35] as an alternative to the bucket technique, with the LR model. This bucketing technique is advised to deal with the heterogeneous subsets in the data [45, 3, 5]. This leads to research question *RQ4*

Then, transparent models (i.e. model that are faithful by design) seem to underperform compared to the black box models in the case of sequential and high-dimensional data [8]. Therefore, research question *RQ5* compares the transparent models with the deep learning models.

The next two research questions are based on the interpretability metrics, and describes the interpretability-accuracy trade-off in OOPPM and difference in the relative ranking of the parsimony and the functional complexity values. Finally, the faithfulness of the post-hoc explanations is compared with explanations that are calculated during the fitting of the black box model. Moreover, it is implicitly assumed that the faithfulness of the latter should be higher compared to the post-hoc explanations. This leads to the research question *RQ8*. The final research question *RQ9* compares the monotonicity with the LOD@10 values.

RQ1. What is the influence of the encoding mechanism on the interpretability of the explanations and faithfulness of the explainability model?

RQ2. Do deep learning models extract more information from the sequential,

control flow perspective compared to the other models which are conceived for tabular data?

RQ3. *Does the previously established outperforming of the deep learning models come at the expense of the interpretability and faithfulness?*

RQ4. *Does the LLM model outperform the logistic regression model?*

RQ5. *Are transparent models capable of attaining the performance level of the black box models in the field of OOPPM?*

RQ6. *Is the relative ranking of parsimony values similar to the ranking of the functional complexity values?*

RQ7. *Does the interpretability-accuracy trade-off holds in the field of OOPPM?*

RQ8. *Are the explanations generated by post-hoc explainability techniques less faithfulness compared to the explanations that contribute to the predictions of the black box model but are typically calculated afterwards?*

RQ9. *Is an explainability model with a low monotonicity value always associated with a high LOD@10 value?*

5.2. Event logs

This study is based on four different real-life event logs that can be found at the website of 4TU Centre for Research Data¹, and are often used in the field of OOPPM [3, 8, 33, 29, 30]. These event logs are split with Linear Temporal Logic (LTL) rules as defined in [3] to obtain objectives for the process. Moreover, the event log is split based on the labelling functions defined by the four LTL rules, therefore creating four different binary prediction tasks. The event log specifications are defined in Table 1.

¹<https://data.4tu.nl/>

The first event log, BPIC2011, describes the medical history of patients from the Gynaecology department of a Dutch Academic hospital. The applied procedures and treatments of the different cases represent the activities in this event log, with the label being either true or false if the LTL rule is violated or not, respectively. The four different LTL rules generated the following event logs: bpic2011(1), bpic2011(2), bpic2011(3) and bpic2011(4). Next, similar trace prefixing and cutting preprocessing steps are performed as in [3].

The BPIC2015 event log assembles events pertaining to the building permit application process from five Dutch municipalities. A single LTL rule is applied on the event log and split for each of the five municipalities. The LTL rule defines that a certain activity *send confirmation receipt* must always be followed by *retrieve missing data* (and not the other way around), where the latter activity has to always be present in the trace if the former was. No trace cutting was performed on this event log.

The sepsis cases event log contain the discharge information of patients with symptoms of sepsis in a Dutch hospital, starting from the admission in the emergency room until the discharge of the patient. Here, the labelling is performed based on the discharge and/or of the patient instead of LTL rules [3].

Production, the last event log contains information about the activities in a manufacturing process, together with the workers and/or machines of the production of the items itself. The labelling function is based on whether the number of work orders rejected is larger than zero or not.

5.3. Benchmark models and explainability models

The wide variety of classifiers and explainability models used for XAI purposes in this study, is depicted in Fig. 3. The first model is the logistic regression model, an often used interpretable predictive technique to model the probability of a discrete variable. The two advanced logistic regression models, LLM and GLRM, are interpretable models that are introduced in [35] in the field of OOPPM. The former clusters the data with a decision tree and builds linear models in the leave nodes. The latter creates binary rules with a generalized

logistic rule model. In conclusion, the former tree models generate their own explanations.

The next two models are ensemble models, i.e. XGBoost (XGB) [52] and

Event log	Traces	Events	Med. length	Max. length	Trunc. length	Var. (after trunc.)	Act. per trace	Stat. cat. levels	Dyn. cat. levels	Var. to inst. ratio	Events over trace	Event to act. ratio	Dyn./stat. ratio
BPIC2011(1)	1140	67480	25	1814	36	815	193	961	290	0.714912	59	3	0.3
BPIC2011(2)	1140	149730	54.5	1814	40	977	251	994	370	0.857018	131	5	0.37
BPIC2011(3)	1121	70546	21	1368	31	793	190	886	283	0.707404	63	3	0.32
BPIC2011(4)	1140	93065	44	1432	40	977	231	993	338	0.857018	82	3	0.34
BPIC2015(1)	696	28775	42	101	40	677	380	19	433	0.972701	41	1	22.79
BPIC2015(2)	753	41202	55	132	40	752	396	7	429	0.998672	55	1	61.29
BPIC2015(3)	1328	57488	42	124	40	1280	380	18	428	0.963855	43	1	23.78
BPIC2015(4)	577	24234	42	82	40	576	319	9	347	0.998267	42	1	38.56
BPIC2015(5)	1051	54562	50	134	40	1048	376	8	420	0.997146	52	1	52.5
SEPSIS(2)	782	10924	13	60	13	656	15	195	38	0.838875	14	1	0.19
SEPSIS(4)	782	12463	13	185	22	709	15	200	40	0.90665	16	2	0.2
Production	220	2489	9	78	23	203	26	37	79	0.922727	11	3	2.14

Table 1: Event log specifications

Random Forest (RF) [53], which are not interpretable models, as the inherent complexity is what bestows their predictive abilities. In the XGBoost model, weak learners are iteratively improved to a final strong learner by incorporating the loss function of the previous weak learner(s). On the other hand, the Random Forest trains a number of decision trees on various subsets of the data. Different to XGBoost, the voting scheme is based on the majority votes of predictions. By contrast to the transparent models, ensemble methods require an explainability model. For this, the ensemble methods are combined with the post-hoc explainability technique SHAP. Moreover, SHAP values are calculations for each instance-attribute combination based on coalitional game theory. Furthermore, a prediction can be explained by assuming that each attribute value is a player in a game, where the prediction is the payout. This model-agnostic technique tells how to fairly distribute the payout among the attributes, as the SHAP values are the average marginal contribution of an attribute value across all possible coalitions.

Next, two different neural network models are discussed. The first model is a recurrent neural network with Long Short-Term Memory (LSTM) [54], with the long-term relations and dependencies encoded in the cell state vectors, designed

to solve the vanishing gradient problem. The advantage of LSTM over classical machine learning models lies in the ability to model time-dependent and sequential data tasks, where the categorical values are encoded in embeddings. The second model is a Convolutional Neural Network (CNN) [55], which is a deep-forward artificial neural network with information flow starting from the input layers, through the hidden layers, until the output layer (therefore only in one direction). Similar to the ensemble methods, the internal representation of a deep neural network (LSTM and CNN), does not allow for inherent explanations of predictions.

The use of attention layers is a model-specific post-hoc explainability technique in the strict sense of the meaning, as attention is contributing to the prediction but typically calculated afterwards to obtain attribute importance scores. These attention layers calculate non-negative weights (multiplied by their corresponding representations) for each input that together sums to one, and finally sums the resulting vectors into a single fixed-length representation [36]. Second,

5.3.1. Preprocessing steps

First, an equivalent train-test split as in [3] is performed. To this end, a temporal train-test split is performed that ensures that the period of training data does not overlap with the period of the test data, while the event of the cases in the train data that did overlap with the test data are cut. Next, the traces are cut with similar upper length as defined in [3]. Then, both the index and aggregation encoding are used to encode the data for the machine learning algorithms. Note that the aggregation encoding is unique to processes, and merits the investigation of a dedicated XAI-based approach, as introduced in this paper. In the study of [3], the index encoding was only used in combination with the prefix model. Second, we chose to use the index encoding without the prefix length bucketing technique, in contrast with [3]. The embedding mechanism is used for categorical attributes in the deep neural networks. Finally, the event logs are filtered out for which the average obtained AUC over all the classifiers was lower than 50 (i.e. *sepsis cases(2)*), as no analysis should be performed

where random luck has a better ability compared to the classifiers in order to distinguish between the classes). For the XAI evaluation, we additionally filtered out the event logs that had an average AUC below 75 (sepsis cases(3) and production). This was to overcome the issue that explainability techniques can only perform well when the original task model is performant enough.

The bidirectional LSTM neural network architecture with attention layer for interpretation purposes stems from [28]. Compared to the original set-up, the numerical attributes are added as input layers to the LSTM model. Finally, the predictive function of [28] is transformed into a binary outcome-oriented prediction by stripping off the final layer and inserting a sigmoid output layer instead. In order to compare, ceteris paribus, the overall performance of the LSTM with the CNN, we ensure that both models have a similar set-up. Therefore, the CNN model start from the same architecture as the LSTM, and the Bidirectional LSTMs are replaced with 1D convolutional layers. Different to the LSTM model, the attention is calculated directly after the input layers and embeddings (similar to [56]), and the kernel size is set to be the same as the length of the sequences and the filter as the length of the concatenated input. Additionally, an extra dense layer with ReLu activation was added before the final dense layer, in order to ensure that the output is correctly linked back to the inputs.

5.4. Attribute Importance

In case of a black box model, the attribute weights of the task model $w_{e,1}, \dots, w_{e,p}$ need to be measured post-hoc, where for tree-based models a naive method exists in counting the number of times the attributes are selected by the individual trees in the ensemble method [57]. As an improvement, the authors suggest a permutation-based approach by looking at the change in accuracy before and after permuting the attribute values. In this paper, the attribute importance for all black box models are calculated similarly, with the use of a perturbation-based method as described in Algorithm 2, where we evaluate the accuracy change using the Root Mean Squared Error (RMSE). Note that some

remarks about this algorithm should be made. First, the attribute importance for the deep learning models is calculated by permuting the original attributes $[x'_1, \dots, x'_d]$ instead of the transformed attributes $[x_1, \dots, x_p]$. This makes sense for the following reason: the monotonicity value compares the importance of the attributes of the task model with the importance of the attributes of the explainability model. To ensure that they are both calculated on the same number of attributes, the attribute importance is calculated with the original attributes, and the attention values are aggregated to obtain the importances for the original attributes.

Algorithm 2 Attribute Importance

Require: *Attributes, AttibyteTypes, Train*

Ensure: *effects*

```

 $z \leftarrow ()$ ,  $effects \leftarrow ()$ ,  $Train \leftarrow [x_{1,1}, \dots, x_{1,p}, \dots, x_{n,1}, \dots x_{n,p}]$ 
for  $j \in Attributes$  do ▷ take only the attributes of type  $t$ 
     $Train_{copy} \leftarrow Copy(Train)$  ▷ copy the train data for each new attribute
     $NewValues \leftarrow ()$ 
     $z \leftarrow \theta(Train[j])$  ▷ all the unique attribute values of that attribute
    for  $i \in Instances$  do
         $Value = Train(i, j)$  ▷ the current attribute value of instance  $i$ 
         $z^* = \{x \in z : x \notin Value\}$  ▷ remove the current value
        if  $length(z^*) \leq 1$  then
             $NewValues[i, j] \leftarrow Value$  ▷ for static attributes
        else
             $NewValues[i, j] \leftarrow Random(z^*)$  ▷ take a random value
         $Train_{copy}[j] \leftarrow RandomValue(z^*)$  ▷ replace with permuted values
         $\hat{y} \leftarrow predict(Train)$ 
         $y^* \leftarrow predict(Train_{copy})$  ▷ predictions after permuting attribute  $x_j$ 
         $effect_j = \sqrt{\frac{(\hat{y} - y^*)^2}{n}}$  ▷ root mean square error
         $effects(j) \leftarrow effect$  ▷ save the effects of all the attributes

```

5.5. hyper optimization details

Finally, a 4-fold cross validation was performed with the use of Distributed Asynchronous Hyper-parameter Optimization [58] for the machine learning models. The hyper optimization for the deep learning models was done by a 10-fold cross validation, as the neural networks need additional evaluation to overcome

the plethora of local minima. For the LR, XGB and RF model, similar hyperparameter settings are taken from [3]. For the LLM model, we additionally incorporate the maximum depth of the decision tree and the minimum samples per leaf to ensure that the tree splitting does not allow overfitting. According to [33], the optimal dropout rate for the bidirectional LSTM with attention was around 0.2. Therefore, we have set the maximal dropout rate to 0.3 (as a margin of error).

As a final remark, extra detailed information about design implementations and parameters are provided on GitHub², to enhance the reproducibility results.

6. Discussion

In the next subsection, the research questions are answered in-depth. To obtain actionable results, it is required that we link the obtained insights with the event log specifications from Table 1. For this, a case-based evaluation in the context of OOPPM is performed with the use of two event logs. This section is finalized with the guidelines for Explainable AI in OOPPM in order to guide the practitioner to the correct model selection.

Event log	LR_{agg}	LR_{index}	LLM_{agg}	LLM_{index}	$GLRM_{agg}$	$GLRM_{index}$	XGB_{agg}	XGB_{index}	RF_{agg}	RF_{index}	$LSTM_{embed}$	CNN_{embed}
BPIC2011(1)	96.60	94.43	96.38	94.79	92.05	81.16	95.57	92.31	93.09	89.42	79.48	76.92
BPIC2011(2)	98.81	96.41	97.23	94.16	97.97	88.11	97.99	90.28	98.49	93.89	89.25	79.20
BPIC2011(3)	98.72	97.21	97.24	96.71	98.39	97.62	98.85	97.70	98.87	96.78	79.69	89.86
BPIC2011(4)	87.77	86.98	88.38	87.24	78.94	78.03	85.12	83.62	89.04	77.53	87.27	83.04
BPIC2015(1)	90.86	88.78	91.34	74.34	88.62	46.96	91.39	74.45	92.53	71.00	91.16	89.01
BPIC2015(2)	95.15	89.58	92.72	90.16	86.53	57.88	94.91	82.87	94.00	87.95	93.62	93.74
BPIC2015(3)	95.85	89.82	95.64	90.53	93.79	55.08	94.93	86.80	95.86	89.54	94.97	94.79
BPIC2015(4)	93.77	93.78	93.71	94.34	91.33	62.98	93.05	81.88	93.98	84.50	91.61	85.05
BPIC2015(5)	93.86	91.48	93.89	90.59	90.49	77.50	94.12	83.18	94.96	89.22	92.94	93.23
SEPSIS(2)	92.79	92.63	89.48	88.18	73.04	73.04	84.92	86.79	82.70	81.97	79.32	84.34

Table 2: Performance(AUC) per Encoding-Classifier Combination

6.1. Research questions

Table 2 gives an overview of the AUC results for the encoding-classifier combinations. To have a more profound idea about the performance per model

²GitHub link is omitted to ensure anonymization

complexity or per sequence encoding mechanisms, we use statistical tests to mathematically ground the conclusions.

First, we investigate whether the model complexity (see Fig. 3) has a significant influence on the performance (AUC). Similar to Kratsch et al. [8], we compare the embedded deep learning models with the index-encoded ensemble methods. The paired t-test ($p_{value} = 0.188$) indicates that the DL models (83.62 AUC) do not statistically outperform the index-encoded ensemble models (83.55 AUC), despite having a slightly higher mean. Comparing Table 1 and Table 2, we indeed can see that deep learning models tend to work best for event logs with a high variant to instance ratio (i.e. BPIC2015(2), BPIC2015(1), BPIC2015(3), BPIC2015(5), BPIC2011(4)). Additionally, we also see that CNN outperforms LSTM for logs featuring a high dynamic versus static ratio (BPIC2015(2) and BPIC2015(5)).

Many papers state that sequence encoding and extraction of attributes is the most important to increase the predictive performance [4, 5]. Moreover, we expect the index encoding to perform better than the aggregation encoding, as the former provides the predictive model with more information about the sequential development of the process. Contrarily, the paired t-test shows that the aggregation encoding (88.47 AUC) statistically outperforms ($p_{value} = 0.003$) the index encoding (83.55 AUC), with the former obtaining the best results in 9 out of 10 event logs. Intuitively, one could argue that the index encoding is potentially underperforming due to an explosion of the attribute space. Next, the use of index encoding over aggregation encoding is expected to increase the parsimony and consequently induce more complex explanations. As an example, Table 3 indeed shows that the parsimony of the event attributes (C_{event}) increased with a factor of 15 for the index-encoded variant of the RF-agg model of the event log BPIC2011(2). In a nutshell, the index encoding has generally higher values for parsimony compared to its aggregation variant. Finally, regarding the faithfulness of the model, we observe that the index-encoding has a negative impact on the monotonicity of the explainability model. Moreover, in only two situations, the monotonicity was lower for the index-encoded variant

(sepsis cases (2) and bpic2011(2)). These observations answer *RQ1*.

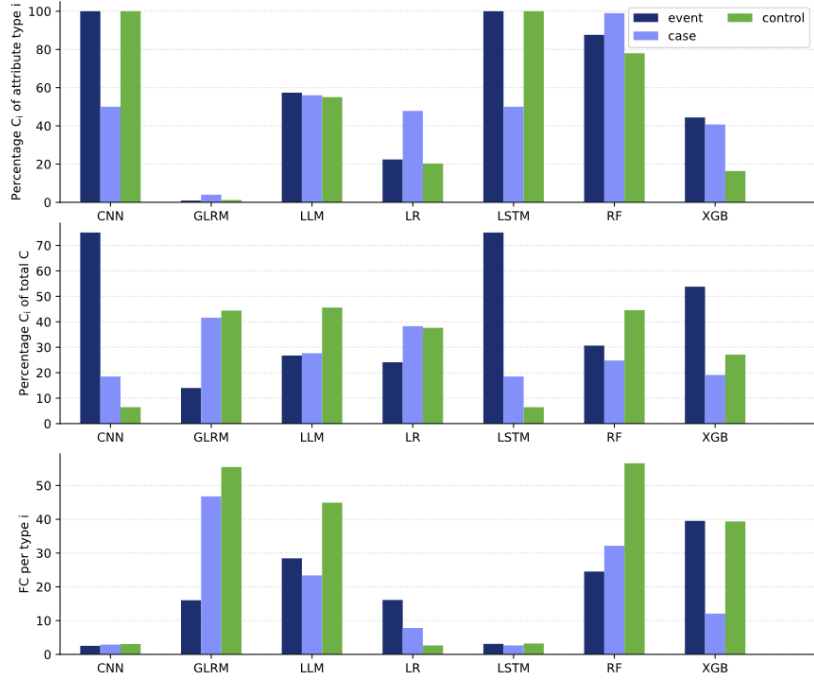


Figure 4: Interpretability metrics per classifier. The top figure describes the percentage of parsimony of each attribute type individually. The second subplot of Fig. 4 shows the percentage parsimony per attribute type, over the total parsimony. The bottom subplot shows the functional complexity per attribute type.

Then, the first subplot of Fig. 4 shows that the deep learning models seem to extract more information from the sequential, control perspective compared to the other models (deep learning models use 100% of the control attributes), answering *RQ2*. If we look at the mean value per dataset (including the aggregation encoding), the bottom-up ranking of the classifiers is as follows: CNN, LSTM, XGB, RF, LLM, LR. This means that two transparent models obtain the highest performance (on average), with the deep learning models having the worst performance. The transparent models are therefore able to attain the performance level of the black box models in the case of sequential and high-dimensional data, already answering *RQ4*. A possible explanation for why the

deep learning models underperform compared to the machine learning models is due to the trace cutting of the prefixes (see Section 3), as the deep learning models are better capable of handling these long-term dependencies. In contradiction with [51], the LSTM neural network seems to have better performance results than the convolutional neural network. Finally, to answer *RQ3*, the functional complexity of the deep learning models is extremely low, which casts considerable doubt on the interpretation of the generated explanations. Next, the faithfulness of the CNN model is very compromised (even reports negative values). This can be due to the fact that attention values focus on explaining the representation of data inside a network rather than explaining the processing of data [59].

Additionally, the logistic regression (outperforming in 4 out of 10 event logs) is higher ranked compared to the LLM model (outperforming LR only for BPIC2015(4)). A possible explanation is that at least one split is *enforced* by the decision tree of the LLM model, regardless of the performance. This answers *RQ5*.

Some additional interesting remarks can be made from Fig. 4. First, even though most of the attributes used in the deep neural networks are event attributes, permuting these values has a very low influence on the predictions. This means that, although indicated as important by the model, the FC shows otherwise. On the other hand, the XGBoost model does not seem to be using a lot of control attributes (noticeable with the top two figures in Fig. 4, but the functional complexity of the respective variables are very high, which means that this attribute type was very important for the prediction. This shows that the relative ranking of the functional complexity values is not always similar to the relative ranking of the parsimony values. Similar insights can also be obtained from Table 3 (BPIC2015(3)), The GLRM model only uses eight control attributes, but permuting them leads to more than 85% different predicted labels. This answers *RQ6*.

To answer the research question *RQ7*, the interpretability-accuracy trade-off does not hold in the field of Outcome-Oriented Predictive Process Monitoring

if we look at the average amount of parsimony versus the average amount of AUC. Moreover, the aggregation encoded (agg-encoded) models seem to obtain higher AUC and report lower parsimony values. Interesting to see is how well the GLRM model performs with an average of 12 attributes (compared to over 625 and 187 for LR and RF respectively), while remaining similarly performant. If we compare the interpretability of the explanations (i.a. defined by the parsimony of the control attributes, C_{ctrl}), then the logistic regression (≈ 100) performs a lot worse than GLRM (≈ 10), but still better than LLM (≈ 600). Furthermore, the XGBoost model seems to obtain higher values (for both event logs in Fig. 3 for monotonicity compared to the LSTM and CNN model, answering *RQ8*. Finally, if we look at BPIC2015(3) and the XGB-agg model in Fig. 3, we can observe a rather high value for monotonicity (0.78), but also a high value for LOD (8.83). This means that the ranking of the importance of all the attributes was rather good, but the SHAP values were not able to indicate correctly on what attribute types the task model XGBoost truly focused, answering *RQ9*.

6.2. Event log Analysis

A more in-depth analysis is given for two event logs, BPIC2015(3) and BPIC2011(2). In BPIC2015(3), all the agg-encoded ML models obtain the best performance, and the DL models outperform the index-encoded ML models (with LSTM outperforming the CNN). This provides insight into the extent to which the outperformance is in trade off with the explainability. Contrarily, the index encoded ML models performed better than the DL models in BPIC2011(2).

First, Table 1 indicates that the BPIC2015(3) event log has a high variant to instance ratio (0.96) and high dynamic vs. static ratio (23.78), the event log properties defined by [8] for which the DL model outperform the ML model. Next, the LTL rule setting the objective is based on the presence of control attributes. Therefore, we expect a high functional complexity value for the control attributes (FC_{ctrl}), which is clearly visible in most of the models. As an

example: the FC_{ctrl} value of the index-encoded LLM model for BPIC2015(3) states that more than 98% of the predictions change after permuting the control attributes. Furthermore, the $\frac{C_{case}}{case}$ values show that most models still use most of the case (i.e. static) attributes, meaning that there is a lot of case-specific information in the event logs.

It is also possible to compare the interpretability between different classifiers.

BPIC2015(3)	AUC	event	case	ctrl	C_{event}	C_{case}	$C_{control}$	$\frac{C_{event}}{event}$	$\frac{C_{case}}{case}$	$\frac{C_{ctrl}}{ctrl}$	FC_{event}	FC_{case}	FC_{ctrl}	Mono.	LOD_{010}
GLRM-index	55.08	1700	34	3083	1	3	9	0.06	8.82	0.29	1.12	97.14	97.31	1.00	0.00
XGB-index	86.8	1700	34	3083	376	21	146	22.12	61.76	4.74	27.78	6.74	46.35	0.78	8.83
RF-index	89.54	1700	34	3083	1317	33	1867	77.47	97.06	60.56	12.76	85.08	85.08	0.17	7.87
LR-index	89.82	1700	34	3083	823	33	1744	48.41	97.06	56.57	18.80	6.10	5.68	1.00	0.00
LLM-index	90.53	1700	34	3083	439.75	11.5	804.5	25.87	33.82	26.09	13.43	0.00	98.05	1.00	0.00
GLRM-agg	93.79	87	34	314	2	1	8	2.30	2.94	2.55	0.00	0.00	85.52	1.00	0.00
CNN-embed	94.79	11	18	1	11	0	1	100.00	0.00	100.00	1.00	1.01	1.15	-0.48	3.74
XGB-agg	94.93	87	34	314	62	21	74	71.26	61.76	23.57	16.88	3.08	87.72	0.87	1.41
LSTM-embed	94.97	11	18	1	11	0	1	100.00	0.00	100.00	2.10	1.17	2.19	0.53	0.00
LLM-agg	95.64	87	34	314	86	33.5	307.5	98.85	98.53	97.93	1.22	0.00	93.09	1.00	0.00
LR-agg	95.85	87	34	314	63	33	160	72.41	97.06	50.96	0.06	0.01	1.30	1.00	0.00
RF-agg	95.86	87	34	314	84	33	275	96.55	97.00	87.58	14.02	5.38	81.89	0.43	10.20
BPIC2011(2)	AUC	event	case	ctrl	C_{event}	C_{case}	$C_{control}$	$\frac{C_{event}}{event}$	$\frac{C_{case}}{case}$	$\frac{C_{control}}{control}$	FC_{event}	FC_{case}	$FC_{control}$	Mono.	LOD_{010}
CNN-embed	79.20	13	6	1	13	6	1	100.00	100.00	100.00	0.51	0.51	0.51	-0.14	3.00
GLRM-index	88.12	2660	760	3139	7	13	8	0.26	1.71	0.25	10.28	27.12	59.92	1.00	0.00
LSTM-embed	89.25	13	6	1	13	6	1	100.00	100.00	100.00	0.23	0.25	0.25	0.61	1.00
XGB-index	90.28	2660	760	3139	308	79	110	11.58	10.39	3.50	21.58	19.46	14.10	0.68	2.45
RF-index	93.89	2660	760	3139	2061	760	1974	77.48	100.00	62.89	15.90	12.34	46.67	0.06	5.10
LLM-index	94.16	2660	760	3139	7.5	28.75	9	0.28	3.78	0.29	40.78	77.80	19.64	1.00	0.00
LR-index	96.41	2660	760	3139	39	148	57	1.47	19.47	1.82	3.67	0.66	0.65	1.00	0.00
LLM-agg	97.23	146	760	215	126.5	542.5	192.5	86.64	71.38	89.53	44.86	0.36	9.07	1.00	0.00
GLRM-agg	97.89	146	760	215	3	20	6	2.05	2.63	2.79	5.01	34.08	45.06	1.00	0.00
XGB-agg	97.99	146	760	215	79	65	73	54.11	8.55	33.95	41.43	13.93	23.61	0.75	2.83
RF-agg	98.49	146	760	215	134	760	207	91.78	100.00	96.28	27.54	28.11	25.33	0.05	8.60
LR-agg	98.81	146	760	215	7	118	9	4.79	15.53	4.19	3.22	0.38	0.54	1.00	0.00

Table 3: The results for BPIC2015(3) and BPIC2011(2). The colours rank the values of each column separately (dark red indicates the worst, dark green the best values). Finally, the higher FC values, the darker the blue.

Moreover, we see a functional complexity of 87.72% for the control attributes of the XGB-agg model, with a parsimony of 74. For the RF-agg model, we observe a functional complexity of 81.89%, with a parsimony of 275 control columns. This means that the XGB-agg model uses fewer attributes compared to RF-agg, but the attributes used are more important for the predictions made (as 87% percent of the predictions change if these attributes are permuted).

From a performance-based perspective, the agg-encoded random forest (RF-agg) model is preferred. Nonetheless, it seems that both the monotonicity and

the LOD@10 values show that the result is compromised. This means that the explainability model is not able to correctly mimic the model behaviour. This can be due to the fact that the random forest model seems to be using all of its attributes (visible with the red colour) based on the values for $\frac{C_{event}}{event}$, $\frac{C_{case}}{case}$ and $\frac{C_{ctrl}}{ctrl}$. The LR-agg model is faithful by definition, as it generates its own explanations. Nonetheless, the model uses 160 control attributes, but only 1.30% of the predictions change when we permute the control attribute values of the test data (*do these 160 attributes really matter for the interpretation of the explanation?*). Next, the LLM-agg model obtains the second-best performance, but has a very low value for interpretability (high parsimony values). A next remark is that, although the LSTM model has a considerably smaller attribute space (as the attention values are for the original attributes due to the embedding mechanism), the monotonicity appears to be compromised.

Finally, the GLRM-agg uses only eight control attributes, two event and one case attribute, while remaining performant (93.79 AUC). The probability of being classified as 'deviant' is calculated in a similar way to logistic regression [35] with the formula:

$$\log(z) = \frac{1}{(1+e^{-z})} \text{ with}$$

$$\begin{aligned} z = & 6.35 - 10.20 * (\neg ctrl1_{agg} \cup ctrl2_{agg} \leq 0.5) - 5.76 * ((ctrl3_{agg} > 0.5) \cup (ctrl2_{agg} \leq 0.50) \\ & - 2.86 * ((ctrl2_{agg} \leq 0.5) \cup (\neg case1)) - 1.34 * (\neg ctrl1_{agg} \cup (ctrl2_{agg} \leq 0.5) \cup (event1 > 7.5)) \\ & - 0.97 * ((ctrl2_{agg} \leq 0.5) \cup (event1 \geq 7.5)) \end{aligned}$$

The rules are roughly based on the presence (or absence) of certain control attributes in combination with another attribute. The use of the GLRM model is advised, as the model is inherently faithful (i.e. creates its own rules) and is highly interpretable while remaining performant in terms of AUC.

Similarly, an analysis for the event log BPIC2011(2) can be made. From a performance-based point of view, the LR-agg is preferred. Nonetheless, it

is again noticeable that the FC_{case} value indicates that less than 1% of the predictions change, despite the model using 118 case attributes. We also observe that the models that a higher value for F_{case} is related with a lower value for monotonicity. It seems that the explainability model is worse in approximating the model behaviour when the task model used a lot of case-specific attributes. This might explain the low monotonicity value for RF, as the BPIC2011(2) event log is indicated by very long traces with a high amount of static categorical values (>670) and RF uses up to 100% of these case variables.

Intuitively, this means that the explainability model is better in approximating

X-MOP: eXplainable models and Metrics in Outcome-oriented predictice Process Monitoring

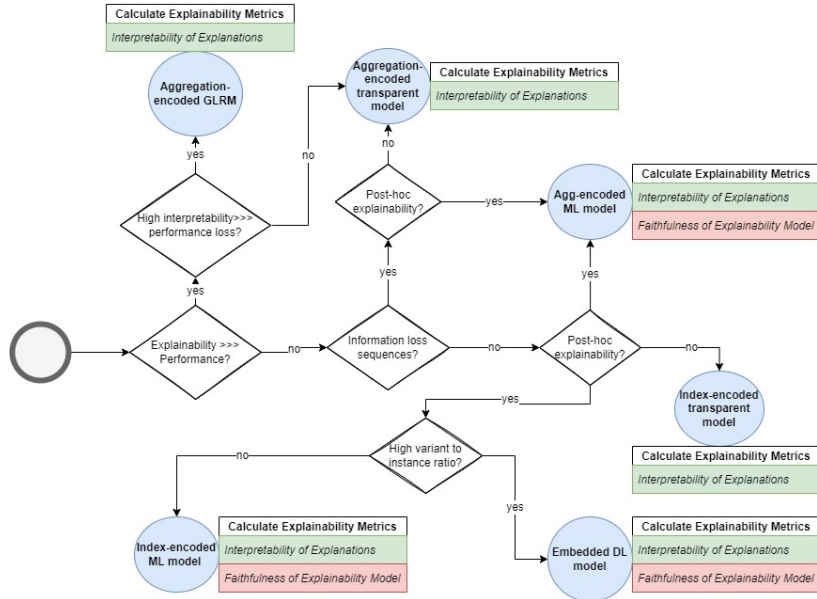


Figure 5: X-MOP: the guidelines for explainable AI purposes in OOPPM

the importance ranking of the attributes used by the task model when the model uses mostly control attributes compared to case attributes. The monotonicity of the model is also high for a higher dynamic vs. static ratio (as explained above), a higher average of activities per trace and a higher number of event

classes.

6.3. *XMOP: Guidelines for XAI in OOPPM*

The obtained insights with the use of the research questions and event log analyses are summarized in an XAI-based guidelines map for OOPPM Fig. 5. This figure describes the guidelines for Explainable AI purposes in OOPPM. The white boxes are the questions to guide partitioners and researchers in obtaining OOPPM results according to their preferences in terms of predictive accuracy and interpretability. The blue circles are the final recommendations for the sequence encoding and model complexity. Note that the guidelines are designed in a very generic way, e.g., no distinction between the LSTM and CNN based on dynamic vs. static ratio. Nonetheless, we specifically recommend the GLRM model when the interpretability of the model is very important (see next subsection for further motivation). Finally, the faithfulness metrics only need to be calculated for non-transparent models,

7. Conclusion

The growing interest in applying machine and deep learning models in OOPPM has fuelled a widespread urge to assess the trustworthiness of predictive models. The contribution made in this paper are threefold. First, we introduce a framework of metrics to evaluate the explainability of predictive models used for OOPPM purposes. Furthermore, we provide an extensive benchmark study of two introduced models versus both transparent and non-transparent models, on which we additionally apply our framework. Not only can we conclude that the transparent GLRM model exhibits very interpretable explanations for high dimensional and sequential data (for only a small loss of performance), but also that the deep learning models tend to underperform. However, the introduced framework shows that the deep neural networks create more interpretable explanations compared to the logistic regression model. Nevertheless, the faithfulness of the logistic regression model is ensured by definition, where

the metrics show how unfaithful the post-hoc explanations for the deep learning models are. Next, in order to provide the reader with a consistent overview of the insights obtained by this study in the field of OOPPM, several hypotheses contrasting traditional machine learning, deep learning, preprocessing and explainability approaches were evaluated on a wide array of transparent and non-transparent models. The results indicate that certain hypotheses (although based on literature) do not apply in the field of OOPPM. In conclusion, we show that each model has its advantages and disadvantages, where naively opting for the model with the highest performance can have a strong detrimental effect on both the interpretability of explanations and the faithfulness of an explainability model. One of the limitations of this research is the fact that the interpretability of the aggregated values (in the case of aggregation encoding) is not taken into account. Therefore, it is assumed that the summary statistics of a certain variable contain no loss in information compared to the original attribute values. Future work will focus on the concept of Responsible AI, by introducing causal inference to assess the causal insights obtainable from predictive models, and focus on the creation of fairness-aware decision models.

References

- [1] M. Dumas, M. L. Rosa, J. Mendling, H. A. Reijers, *Fundamentals of Business Process Management*, Second Edition, Springer, 2018.
- [2] M. Dumas, M. La Rosa, J. Mendling, H. A. Reijers, et al., *Fundamentals of business process management*, Vol. 1, Springer, 2013.
- [3] I. Teinemaa, M. Dumas, M. L. Rosa, F. M. Maggi, *Outcome-oriented predictive process monitoring: Review and benchmark*, *ACM Trans. Knowl. Discov. Data* 13 (2) (2019) 17:1–17:57.
- [4] A. Senderovich, C. Di Francescomarino, C. Ghidini, K. Jorbina, F. M. Maggi, *Intra and inter-case features in predictive process monitoring: A*

tale of two dimensions, in: International Conference on Business Process Management, Springer, 2017, pp. 306–323.

- [5] I. Verenich, M. Dumas, M. La Rosa, F. M. Maggi, C. Di Francescomarino, Complex symbolic sequence clustering and multiple classifiers for predictive process monitoring, in: International Conference on Business Process Management, Springer, 2016, pp. 218–229.
- [6] M. de Leoni, W. M. P. van der Aalst, M. Dees, A general process mining framework for correlating, predicting and clustering dynamic behavior based on event logs, *Inf. Syst.* 56 (2016) 235–257.
- [7] P. De Koninck, S. vanden Broucke, J. De Weerdt, act2vec, trace2vec, log2vec, and model2vec: Representation learning for business processes, in: International Conference on Business Process Management, Springer, 2018, pp. 305–321.
- [8] W. Kratsch, J. Manderscheid, M. Röglinger, J. Seyfried, Machine learning in business process monitoring: a comparison of deep learning and classical approaches used for outcome prediction, *Business & Information Systems Engineering* (2020) 1–16.
- [9] K. Heinrich, P. Zschech, C. Janiesch, M. Bonin, Process data properties matter: Introducing gated convolutional neural networks (gcnn) and key-value-predict attention networks (kvp) for next event prediction with deep learning, *Decision Support Systems* 143 (2021) 113494.
- [10] J. Evermann, J.-R. Rehse, P. Fettke, Predicting process behaviour using deep learning, *Decision Support Systems* 100 (2017) 129–140.
- [11] S. Pauwels, T. Calders, Bayesian network based predictions of business processes, in: International Conference on Business Process Management, Springer, 2020, pp. 159–175.
- [12] A. B. Arrieta, N. D. Rodríguez, J. D. Ser, A. Bennetot, S. Tabik, A. Barbadó, S. García, S. Gil-López, D. Molina, R. Benjamins, R. Chatila, F. Her-

- ra, Explainable artificial intelligence (XAI): concepts, taxonomies, opportunities and challenges toward responsible AI, *Inf. Fusion* 58 (2020) 82–115. [doi:10.1016/j.inffus.2019.12.012](https://doi.org/10.1016/j.inffus.2019.12.012).
- [13] C. Rudin, Stop explaining black box machine learning models for high stakes decisions and use interpretable models instead, *Nature Machine Intelligence* 1 (5) (2019) 206–215.
- [14] A. F. Markus, J. A. Kors, P. R. Rijnbeek, The role of explainability in creating trustworthy artificial intelligence for health care: A comprehensive survey of the terminology, design choices, and evaluation strategies, *J. Biomed. Informatics* 113 (2021) 103655.
- [15] J. Zhou, A. H. Gandomi, F. Chen, A. Holzinger, Evaluating the quality of machine learning explanations: A survey on methods and metrics, *Electronics* 10 (5) (2021) 593.
- [16] C. Rudin, B. Ustun, Optimized scoring systems: Toward trust in machine learning for healthcare and criminal justice, *Interfaces* 48 (5) (2018) 449–466.
- [17] C. Rudin, C. Wang, B. Coker, The age of secrecy and unfairness in recidivism prediction, *Harvard Data Science Review* 2 (1), <https://hdsr.mitpress.mit.edu/pub/7z10o269> (3 2020). [doi:10.1162/99608f92.6ed64b30](https://doi.org/10.1162/99608f92.6ed64b30).
URL <https://hdsr.mitpress.mit.edu/pub/7z10o269>
- [18] I. Nunes, D. Jannach, A systematic review and taxonomy of explanations in decision support and recommender systems, *User Modeling and User-Adapted Interaction* 27 (3) (2017) 393–444.
- [19] V. Pasquadibisceglie, G. Castellano, A. Appice, D. Malerba, Fox: a neuro-fuzzy model for process outcome prediction and explanation, in: 2021 3rd International Conference on Process Mining (ICPM), IEEE, 2021, pp. 112–119.

- [20] C. Rudin, C. Chen, Z. Chen, H. Huang, L. Semenova, C. Zhong, Interpretable machine learning: Fundamental principles and 10 grand challenges, CoRR abs/2103.11251 (2021).
- [21] M. Velmurugan, C. Ouyang, C. Moreira, R. Sindhgatta, Evaluating fidelity of explainable methods for predictive process analytics, in: International Conference on Advanced Information Systems Engineering, Springer, 2021, pp. 64–72.
- [22] R. Sindhgatta, C. Ouyang, C. Moreira, Exploring interpretability for predictive process analytics, in: ICSOC, Vol. 12571 of Lecture Notes in Computer Science, Springer, 2020, pp. 439–447.
- [23] W. Rizzi, C. D. Francescomarino, F. M. Maggi, Explainability in predictive process monitoring: When understanding helps improving, in: BPM (Forum), Vol. 392 of Lecture Notes in Business Information Processing, Springer, 2020, pp. 141–158.
- [24] N. Tax, I. Verenich, M. L. Rosa, M. Dumas, Predictive business process monitoring with LSTM neural networks, in: CAiSE, Vol. 10253 of Lecture Notes in Computer Science, Springer, 2017, pp. 477–492.
- [25] M. Hinkka, T. Lehto, K. Heljanko, A. Jung, Classifying process instances using recurrent neural networks, in: International Conference on Business Process Management, Springer, 2018, pp. 313–324.
- [26] E. Rama-Maneiro, J. C. Vidal, M. Lama, Deep learning for predictive business process monitoring: Review and benchmark, CoRR abs/2009.13251 (2020).
- [27] R. Galanti, B. Coma-Puig, M. de Leoni, J. Carmona, N. Navarin, Explainable predictive process monitoring, in: ICPM, IEEE, 2020, pp. 1–8.
- [28] R. Sindhgatta, C. Moreira, C. Ouyang, A. Barros, Exploring interpretable predictive models for business processes, in: BPM, Vol. 12168 of Lecture Notes in Computer Science, Springer, 2020, pp. 257–272.

- [29] M. Harl, S. Weinzierl, M. Stierle, M. Matzner, Explainable predictive business process monitoring using gated graph neural networks, *Journal of Decision Systems* (2020) 1–16.
- [30] N. Mehdiyev, P. Fettke, Explainable artificial intelligence for process mining: A general overview and application of a novel local explanation approach for predictive process monitoring, *Interpretable Artificial Intelligence: A Perspective of Granular Computing* (2021) 1–28.
- [31] S. M. Lundberg, S. Lee, A unified approach to interpreting model predictions, in: I. Guyon, U. von Luxburg, S. Bengio, H. M. Wallach, R. Fergus, S. V. N. Vishwanathan, R. Garnett (Eds.), *Advances in Neural Information Processing Systems 30: Annual Conference on Neural Information Processing Systems 2017, December 4-9, 2017, Long Beach, CA, USA*, 2017, pp. 4765–4774.
 URL <https://proceedings.neurips.cc/paper/2017/hash/8a20a8621978632d76c43dfd28b67767-Abstract.html>
- [32] M. T. Ribeiro, S. Singh, C. Guestrin, ”why should I trust you?”: Explaining the predictions of any classifier, in: B. Krishnapuram, M. Shah, A. J. Smola, C. C. Aggarwal, D. Shen, R. Rastogi (Eds.), *Proceedings of the 22nd ACM SIGKDD International Conference on Knowledge Discovery and Data Mining, San Francisco, CA, USA, August 13-17, 2016*, ACM, 2016, pp. 1135–1144. doi:10.1145/2939672.2939778.
 URL <https://doi.org/10.1145/2939672.2939778>
- [33] J. Wang, D. Yu, C. Liu, X. Sun, Outcome-oriented predictive process monitoring with attention-based bidirectional lstm neural networks, in: *2019 IEEE International Conference on Web Services (ICWS)*, IEEE, 2019, pp. 360–367.
- [34] V. Pasqualebisceglie, A. Appice, G. Castellano, D. Malerba, Using convolutional neural networks for predictive process analytics, in: *2019 international conference on process mining (ICPM)*, IEEE, 2019, pp. 129–136.

- [35] A. Stevens, J. D. Smedt, J. Peeperkorn, Quantifying explainability in outcome-oriented predictive process monitoring, in: J. Munoz-Gama, X. Lu (Eds.), Process Mining Workshops - ICPM 2021 International Workshops, Eindhoven, The Netherlands, October 31 - November 4, 2021, Revised Selected Papers, Vol. 433 of Lecture Notes in Business Information Processing, Springer, 2021, pp. 194–206. doi:10.1007/978-3-030-98581-3_15. URL https://doi.org/10.1007/978-3-030-98581-3_15
- [36] S. Serrano, N. A. Smith, Is attention interpretable?, in: Proceedings of the 57th Annual Meeting of the Association for Computational Linguistics, Association for Computational Linguistics, Florence, Italy, 2019, pp. 2931–2951. doi:10.18653/v1/P19-1282. URL <https://aclanthology.org/P19-1282>
- [37] S. Ma, R. Tourani, Predictive and causal implications of using shapley value for model interpretation, in: Proceedings of the 2020 KDD Workshop on Causal Discovery, PMLR, 2020, pp. 23–38.
- [38] S. Jain, B. C. Wallace, Attention is not explanation, arXiv preprint arXiv:1902.10186 (2019).
- [39] C. Molnar, G. Casalicchio, B. Bischl, Quantifying model complexity via functional decomposition for better post-hoc interpretability, in: PKDD/ECML Workshops (1), Vol. 1167 of Communications in Computer and Information Science, Springer, 2019, pp. 193–204.
- [40] S. R. Islam, W. Eberle, S. K. Ghafoor, Towards quantification of explainability in explainable artificial intelligence methods, in: R. Barták, E. Bell (Eds.), Proceedings of the Thirty-Third International Florida Artificial Intelligence Research Society Conference, May 17-20, 2020, AAAI Press, 2020, pp. 75–81.
- [41] A. Nguyen, M. R. Martínez, On quantitative aspects of model interpretability, CoRR abs/2007.07584 (2020).

- [42] G. A. Miller, The magical number seven, plus or minus two: Some limits on our capacity for processing information., *Psychological review* 63 (2) (1956) 81.
- [43] A. E. Roth, *The Shapley value: essays in honor of Lloyd S. Shapley*, Cambridge University Press, 1988.
- [44] W. M. P. van der Aalst, *Process Mining - Data Science in Action*, Second Edition, Springer, 2016.
- [45] C. Di Francescomarino, M. Dumas, F. M. Maggi, I. Teinemaa, Clustering-based predictive process monitoring, *IEEE transactions on services computing* 12 (6) (2016) 896–909.
- [46] B. F. van Dongen, R. A. Crooy, W. M. van der Aalst, Cycle time prediction: When will this case finally be finished?, in: *OTM Confederated International Conferences” On the Move to Meaningful Internet Systems”*, Springer, 2008, pp. 319–336.
- [47] F. M. Maggi, C. D. Francescomarino, M. Dumas, C. Ghidini, Predictive monitoring of business processes, in: *CAiSE*, Vol. 8484 of *Lecture Notes in Computer Science*, Springer, 2014, pp. 457–472.
- [48] G. T. Lakshmanan, S. Duan, P. T. Keyser, F. Curbura, R. Khalaf, Predictive analytics for semi-structured case oriented business processes, in: *Business Process Management Workshops*, Vol. 66 of *Lecture Notes in Business Information Processing*, Springer, 2010, pp. 640–651.
- [49] A. Ghorbani, A. Abid, J. Zou, Interpretation of neural networks is fragile, in: *Proceedings of the AAAI Conference on Artificial Intelligence*, Vol. 33, 2019, pp. 3681–3688.
- [50] H. Lakkaraju, E. Kamar, R. Caruana, J. Leskovec, Interpretable & explorable approximations of black box models, *CoRR* abs/1707.01154 (2017). [arXiv:1707.01154](http://arxiv.org/abs/1707.01154)
URL <http://arxiv.org/abs/1707.01154>

- [51] H. Weytjens, J. D. Weerdt, Process outcome prediction: Cnn vs. lstm (with attention), in: International Conference on Business Process Management, Springer, 2020, pp. 321–333.
- [52] T. Chen, C. Guestrin, Xgboost: A scalable tree boosting system, CoRR abs/1603.02754 (2016).
- [53] L. Breiman, Random forests, Machine learning 45 (1) (2001) 5–32.
- [54] S. Hochreiter, J. Schmidhuber, Long short-term memory, Neural computation 9 (8) (1997) 1735–1780.
- [55] Y. LeCun, L. Bottou, Y. Bengio, P. Haffner, Gradient-based learning applied to document recognition, Proceedings of the IEEE 86 (11) (1998) 2278–2324.
- [56] W. Yin, H. Schütze, B. Xiang, B. Zhou, Abcnn: Attention-based convolutional neural network for modeling sentence pairs, Transactions of the Association for Computational Linguistics 4 (2016) 259–272.
- [57] C. Strobl, A.-L. Boulesteix, A. Zeileis, T. Hothorn, Bias in random forest variable importance measures: Illustrations, sources and a solution, BMC bioinformatics 8 (1) (2007) 1–21.
- [58] J. Bergstra, R. Bardenet, Y. Bengio, B. Kégl, Algorithms for hyperparameter optimization, Advances in neural information processing systems 24 (2011).
- [59] L. H. Gilpin, D. Bau, B. Z. Yuan, A. Bajwa, M. Specter, L. Kagal, Explaining explanations: An overview of interpretability of machine learning, in: DSAA, IEEE, 2018, pp. 80–89.